Supporting Information

Currat and Excoffier 10.1073/pnas.1107450108

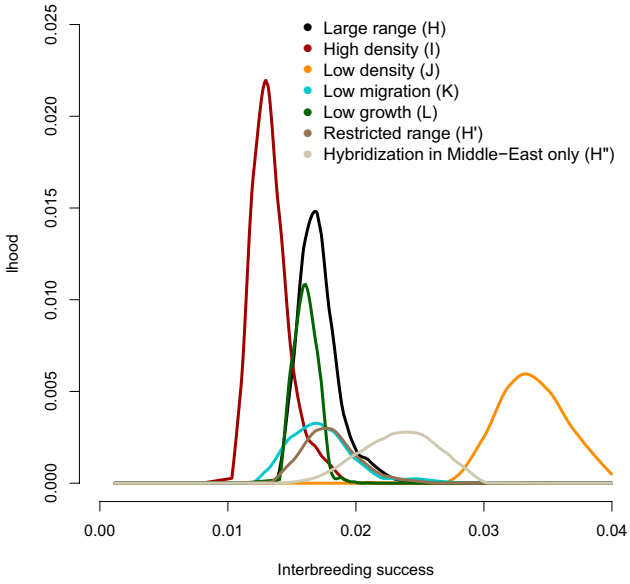

Fig. S1. Distribution of the proportion of simulations (among 10,000) resulting in Neanderthal introgression levels compatible with observations (1.9–3.1%) in French and Chinese samples. Each curve corresponds to a different demographic scenario (defined in Table S1) simulated assuming a deme area of 50×50 km^2. lhood, likelihood.

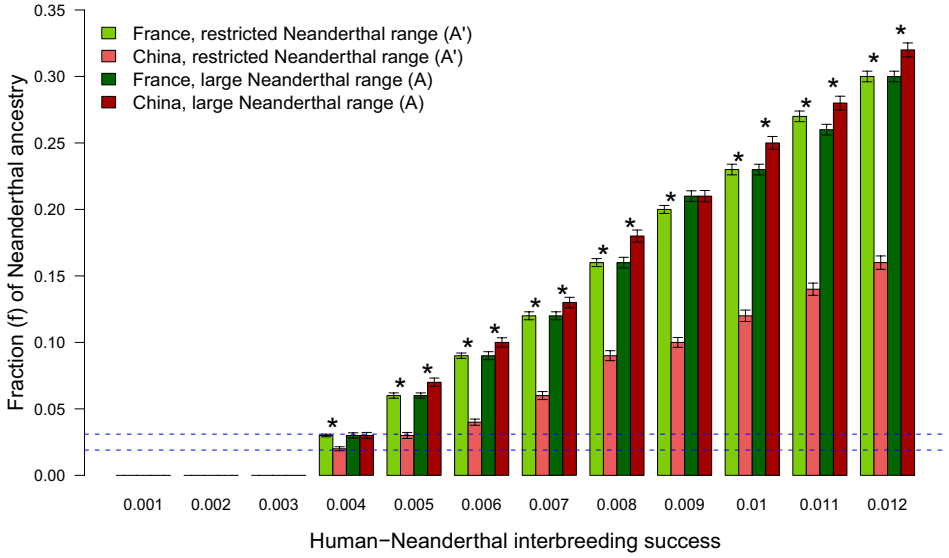

Fig. S2. Average fraction (introgression) of Neanderthal genes in present-day human populations sampled in France (green) and in China (red). Results are based on 10,000 simulations of the ancestry of 100 genes per population. The two light bars on the left are for results obtained under the restricted Neanderthal range (scenario A′), and the two dark bars on the right are for results obtained assuming a large Neanderthal range (scenario A, Fig. 1). Asterisks (*) indicate significantly different Neanderthal ancestry in France and China ($P < 5\%$, t test). The blue dashed lines delimit the assumed range of observed Neanderthal introgression in Eurasians (1.9–3.1%). The parameters used correspond to scenario A in Table 1.

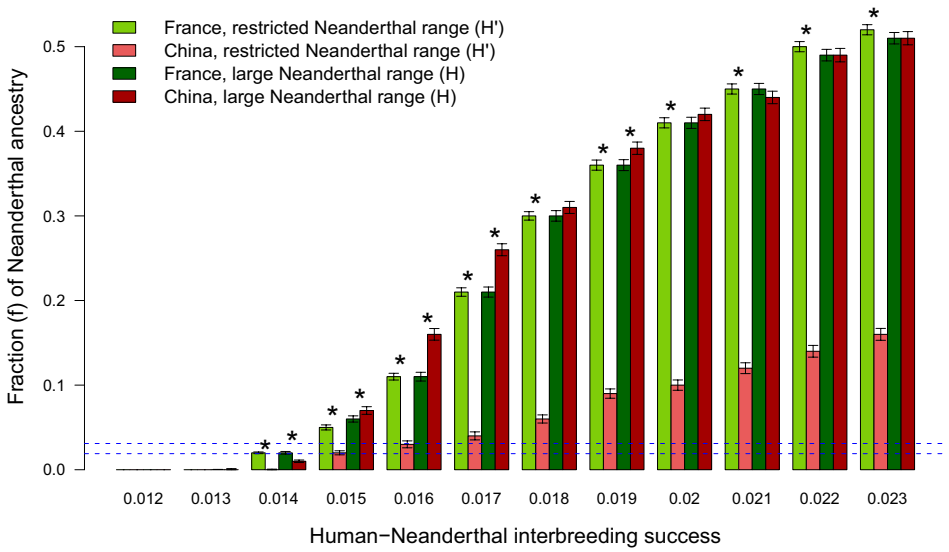

Fig. S3. Fraction (introgression) of Neanderthal genes in present-day human populations sampled in France (red) and in China (green). Results are based on 10,000 simulations of the ancestry of 100 genes per population. Light colors are for results obtained under the restricted Neanderthal range (scenario H′), and dark colors are for results obtained under the large Neanderthal range (scenario H, Fig. 1). Asterisks (*) indicate significantly different Neanderthal ancestry in France and China ($P < 5\%$, t test). The blue dashed lines delimit the assumed range of observed Neanderthal introgression in Eurasians (1.9–3.1%). The parameters used correspond to scenario H in Table S1. Note that these results have been obtained for a deme area of 50×50 km^2.

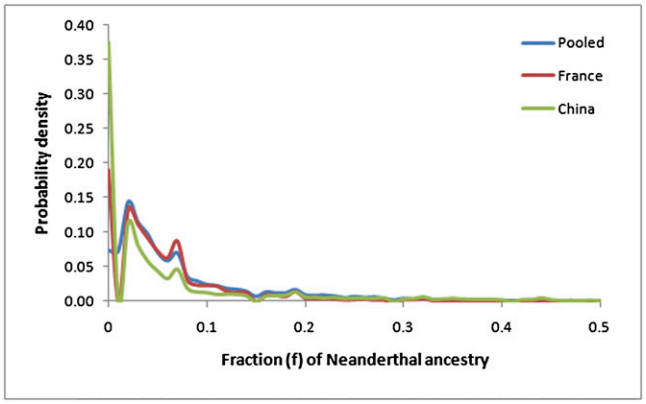

Fig. S4. Probability density of the fraction of Neanderthal ancestry obtained from 10,000 simulations under scenario A and an interbreeding success rate of 0.005. We report the distribution of introgression rates for the French (red) and the Chinese (green) samples separately, as well as for the two samples pooled together (blue).

Table S1. Additional demographic parameters and simulation results for scenarios where simulated deme area is 50 × 50 km²

Scenarios	K_N*	K_H†	r‡	m_N§	m_H¶	Colonization time‖	Interbreeding success**	Model A relative probability††
H: Large Neanderthal range	50	200	0.8	0.25	0.5	260	0.0168 (0.0144–0.0197)	1.86
H′: Restricted Neanderthal range	50	200	0.8	0.25	0.5	260	0.0177 (0.0140–0.0220)	9.20
H′′: Hybridization in Middle East only	50	200	0.8	0.25	0.5	230	0.0241 (0.0173–0.0292)	9.88
I: Large *K*	100	400	0.8	0.25	0.5	260	0.0130 (0.0108–0.0159)	1.25
J: Small *K*	25	100	0.8	0.25	0.5	260	0.0333 (0.0285–0.0391)	4.62
K: Small *m*	50	200	0.8	0.125	0.25	370	0.0170 (0.0128–0.0213)	8.42
L: Small *r*	50	200	0.4	0.25	0.5	370	0.0161 (0.0144–0.0179)	2.54

Except for scenarios H′ (Fig. 1, brown and green areas) and H′′ (Fig. 1, brown area only), hybridization could occur over the whole Neanderthal range shown in Fig. 1. Demographic parameters for scenario H are judged to be the most plausible for this deme area, given our review of the literature.

*Neanderthal carrying capacity.

†Human carrying capacity.

‡Intrinsic rate of growth.

§Migration rate between Neanderthal demes.

¶Migration rate between human demes.

‖Approximate time (in generations) for the colonization of Europe from the Middle East estimated from the simulations. This statistic is determined by the growth and migration rates, and it also varies slightly with the hybridization rate.

**Maximum-likelihood estimates of interbreeding success between humans and Neanderthals are reported with limits of a 95% confidence interval within brackets.

††Probability of scenario A in Table 1 (assuming a resolution of 100 × 100 km²), relative to the other scenarios computed from weighted AICs (*Material and Methods*).